Fast Synthesis of Thiolated Au25 Nanoclusters via Protection–Deprotection Method

ARTICLE *in* JOURNAL OF PHYSICAL CHEMISTRY LETTERS · SEPTEMBER 2012

Impact Factor: 7.46 · DOI: 10.1021/jz300960b

5 AUTHORS, INCLUDING:

Xun Yuan
Institute of Bioengineering and Nanotechnology
40 PUBLICATIONS **1,258** CITATIONS
SEE PROFILE

Yong Yu
Agency for Science, Technology and Research …
23 PUBLICATIONS **626** CITATIONS
SEE PROFILE

Qingbo Zhang
Rice University
34 PUBLICATIONS **2,389** CITATIONS
SEE PROFILE

Jianping Xie
National University of Singapore
110 PUBLICATIONS **4,402** CITATIONS
SEE PROFILE

THE JOURNAL OF PHYSICAL CHEMISTRY Letters

Letter

pubs.acs.org/JPCL

Fast Synthesis of Thiolated Au_{25} Nanoclusters via Protection–Deprotection Method

Xun Yuan, Yong Yu, Qiaofeng Yao, Qingbo Zhang, and Jianping Xie*

Department of Chemical and Biomolecular Engineering, National University of Singapore, 4 Engineering Drive 4, 117576, Singapore

Supporting Information

ABSTRACT: This letter reports a new synthesis strategy for atomically precise Au nanoclusters (NCs) by using a protection–deprotection method. The key in our synthesis strategy is to introduce a surfactant molecule to protect thiolate-Au^I complexes during their reduction. The protecting layer provides a good steric hindrance and controls the formation rate of thiolated Au NCs, which leads to the direct formation of atomically precise Au NCs inside the protecting layer. The protecting layer was then removed from the surface of thiolated Au NCs to bring back the original functional groups on the NCs. The protection–deprotection method is simple and facile and can synthesize high-purity thiolated Au_{25} NCs *within* 10 min. Our synthesis protocol is fairly generic and can be easily extended to prepare Au_{25} NCs protected by other thiolate ligands.

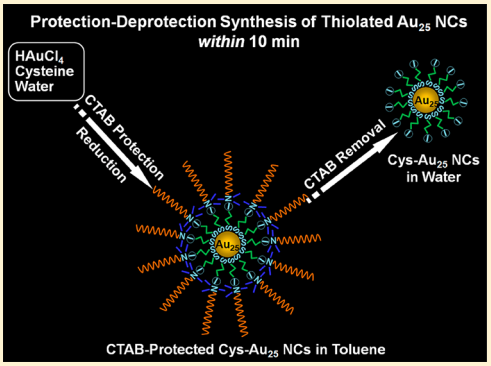

SECTION: Physical Processes in Nanomaterials and Nanostructures

To obtain chemoselectivity in a chemical reaction in organic synthesis, a protecting group is introduced into a molecule by chemical modification of a functional group.[1,2] After the reaction, a deprotection step is used to remove the protecting group, giving back the original functional group. This protection–deprotection strategy plays an important role in multistep organic synthesis.[3] Inspired by this synthesis strategy, here we report a paradigm shift synthesis strategy for noble-metal nanoparticles, where a protection–deprotection sequence is used to facilitate a facile and fast (<10 min) synthesis of atomically precise metal NCs. The key strategy is to introduce a surfactant molecule to protect metal ion precursors (thiolate-Au^I complexes for example) under the harsh reduction condition (e.g., with strong reducing agent sodium borohydride, $NaBH_4$), which controls the formation rate of NCs inside the surfactant templates, thus leading to a direct formation of atomically precise metal NCs within *minutes*. The protecting surfactant molecules can then be removed from the as-formed metal NCs, bringing back the original functional groups on the NC surface.

As a reaction model, we have chosen Au NCs, which typically contain several to one hundred Au atoms.[4−6] Au NCs represent a missing link between single Au atoms and large Au nanocrystals (>2 nm). NCs in this sub-2-nm size regime display discrete electronic transitions and exhibit interesting molecule-like properties,[7−9] such as quantized charging[10−12] and luminescence.[13−17] Facile synthesis of atomically precise Au NCs is the most important step to realizing their practical applications in areas such as biomedical and catalysis.[6,18,19] Two main strategies have been developed so far for the synthesis of atomically precise Au NCs. The first strategy relies on the use of specific capping agents − thiolate ligands, which have unique interactions with Au surface via the thiolate-Au bonds, leading to the formation of Au NCs protected by thiolate ligands (denoted as thiolated Au NCs).[4,5,20−24] Similar to the Ostwald or digestive ripening process in the synthesis of monodisperse Au nanoparticles, a "size focusing" process, typically driven by the unique interactions between thiolate ligands and Au atoms, is required for the preparation of atomically precise thiolated Au NCs.[25−32] The "size focusing" process for thiolated Au NCs generally needs a long time (>24 h) to achieve a good monodispersity.[33] The second approach is the template-directed synthesis. Here macromolecules, such as proteins,[34−37] polymers,[38] and dendrimers,[39] are used as a template to direct the formation of Au NCs. The as-formed Au NCs are embedded inside the cavities of macromolecules and stabilized by the steric hindrance provided by the template molecules. However, the bulky template molecules are difficult or impossible to be removed from the Au NC surface after the reaction, which may limit their practical usability if the template molecules could affect the performance of the embedded Au NCs.

We hypothesized that if we can integrate these two synthesis strategies into one protocol and take advantage of both unique thiolate–Au interactions and steric hindrance of the templates for the formation of Au NCs, then we may develop an efficient and facile synthesis strategy for atomically precise Au NCs. A removable template is another important consideration in our design, which could further improve the versatility and

Received: July 16, 2012
Accepted: August 8, 2012
Published: August 8, 2012

   dx.doi.org/10.1021/jz300960b | *J. Phys. Chem. Lett.* 2012, 3, 2310–2314

Scheme 1. Schematic Illustration of the Fast (<10 min) Synthesis of Cys-Au_{25} NCs by the Protection−Deprotection Method

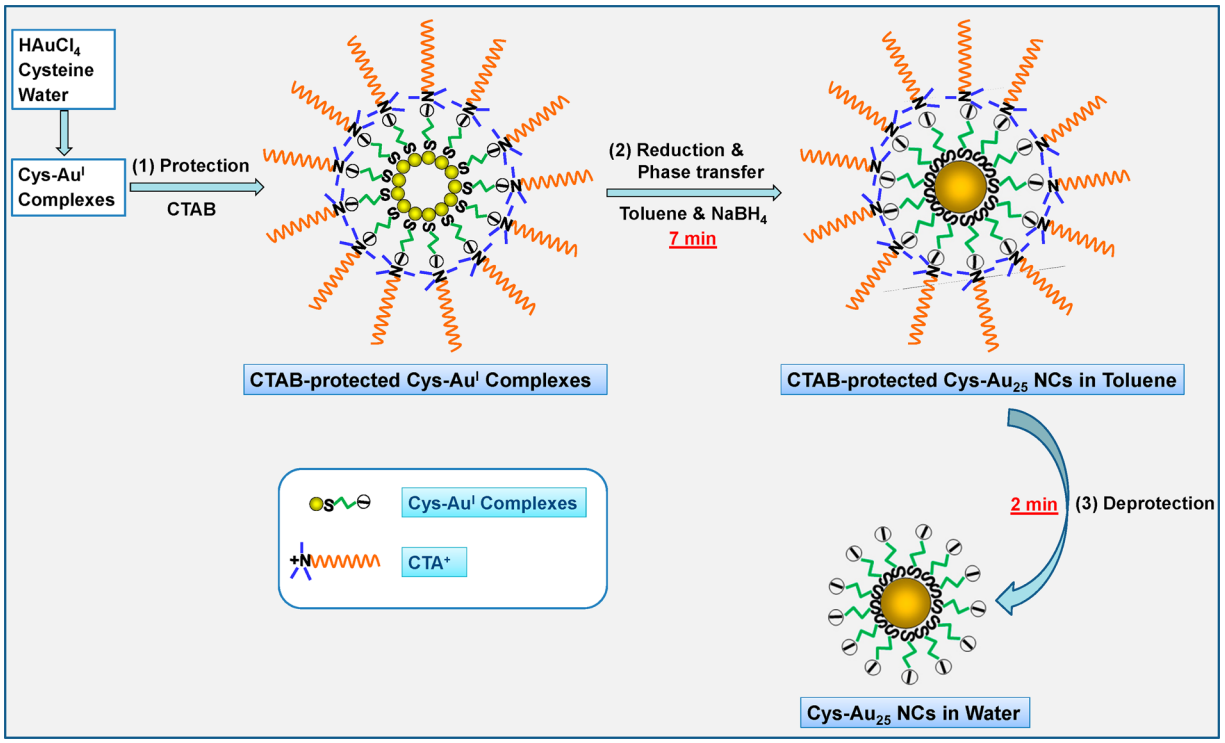

extendability of our synthesis strategy for metal NCs. Here we report such synthesis strategy for the preparation of atomically precise thiolated Au NCs based on a protection−deprotection scheme. As a proof-of-concept, thiolated Au_{25} NCs have been simply synthesized by our method in less than 10 min.

Our synthesis protocol involves three steps. As shown in Scheme 1, the first step is to introduce a surfactant (e.g., cetyltrimethyl ammonium bromide (CTAB)) as a protecting layer for a common Au ion precursor − thiolate-Au^I complexes. A natural thiol-containing amino acid, cysteine (Cys), was selected as our model thiolate ligand. Upon the addition of CTAB into the thiolate-Au^I (or Cys-Au^I) complexes, the positively charged cation (CTA^+) bound to the negatively charged carboxyl group (Cys has one carboxyl group) in the Cys-Au^I complexes via the formation of $(CTA)^+(COO)^-$ ion pairs. The combination of the electrostatic interaction[40,41] (CTA^+ with Cys-Au^I complexes) and the steric hindrance from the surfactant molecules led to the inverse-micelle formation of CTAB-protected Cys-Au^I complexes (Scheme 1).

The second step is the reduction of the CTAB-protected Cys-Au^I complexes to form Cys-protected Au NCs (or Cys-Au NCs), followed by the transfer of the as-formed Au NCs from the aqueous to organic phase. As shown in Scheme 1, when $NaBH_4$ was introduced into the reaction mixture, it diffused inside the inverse-micelles, reduced the Cys-Au^I complexes, and resulted in the formation of Cys-Au NCs, which are protected by a CTAB layer (CTAB-protected Cys-Au NCs in Scheme 1). The introduction of toluene quickly transferred the CTAB-protected Cys-Au NCs from the aqueous to organic phase. The third step is the removal of the protecting CTAB layer from the Cys-Au NC surface. Upon the addition of a hydrophobic anionic surfactant, tetramethylammonium decanoate (TMAD), to the CTAB-protected Cys-Au NCs in toluene, the hydrophobic decanoate anion D^- extracted the hydrophobic cation CTA^+ on the surface of Cys-Au NCs via the formation of hydrophobic $(CTA)^+(D)^-$ ion pairs.[17,42,43] The removal of the hydrophobic cation CTA^+ from Cys-Au NCs brings back the negative charge (from the carboxyl group of Cys) on the Au NCs, shuttling back these NCs to the aqueous phase (Scheme 1).

The synthesis protocol for Cys-Au_{25} NCs is very simple. In a typical synthesis, aqueous solutions of Cys (5 mM, 2 mL) and $HAuCl_4$ (20 mM, 250 μL), ethanolic CTAB (100 mM, 5 mL), NaOH (1 M, 350 μL), toluene (2 mL), and $NaBH_4$ (112 mM, 100 μL) were introduced sequentially into 3 mL of water under vigorous stirring, and the reaction was allowed to proceed for ~7 min. The reddish-brown Au NCs were then observed from the toluene phase. Au NCs in toluene were collected and examined by UV−vis spectroscopy. As shown in Figure 1a (red line), the as-formed Au NCs in toluene show four distinct absorption peaks at 440, 545, 670, and 780 nm, which

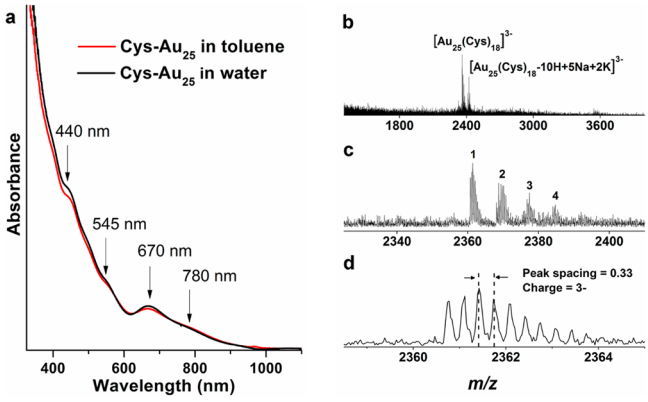

Figure 1. (a) UV−vis spectra of the as-synthesized Cys-Au_{25} NCs in toluene (red line) and in water (black line). (b−d) ESI mass spectra of the as-synthesized Cys-Au_{25} NCs in water (in negative ion mode).

dx.doi.org/10.1021/jz300960b | J. Phys. Chem. Lett. 2012, 3, 2310−2314

correspond well to the characteristic absorption of thiolated Au_{25} NCs.[8] The Au NCs in toluene can be easily transferred back to water by the removal of the protecting CTAB layer on the NC surface. The UV−vis spectrum of Cys-Au NCs in water (black line) shows identical optical absorption as that of Cys-Au NCs in toluene (red line). The well-defined absorption spectra for both Cys-Au NCs in toluene (CTAB-protected) and in water (CTAB-deprotected) suggest a very high purity of Cys-Au_{25} NCs in our crude product.

Electrospray ionization mass spectrometry (ESI-MS) was then used to determine the molecular formula of our Cys-Au NCs. As shown in Figure 1b, the ESI mass spectrum of Cys-Au NCs in water shows two set of intense peaks at ~m/z 2361 and 2423 in the 1300−4000 range, which can be assigned to $[Au_{25}(Cys)_{18} - 3H]^{3-}$ and $[Au_{25}(Cys)_{18} - 10H + 5Na + 2K]^{3-}$, respectively. (See the detailed assignment as following.) For example, the zoom-in spectrum in Figure 1c indicates that the base peak at m/z 2361.42 (#1) is accompanied by a group of similar peaks (#2−#4) spaced m/z 7.3 apart, which is a typical mass difference of a H^+ dissociation and a Na^+ coordination [−H + Na] divided by three charges.[44] The ionized Cys-Au NCs carry three negative charges, as indicated by its isotopic pattern at m/z 2361.42 (Figure 1d), which has an isotopic peak spacing of 0.33. Other identifiable species in Figure 1c are $[Au_{25}(Cys)_{18} - 4H + Na]^{3-}$ (#2), $[Au_{25}(Cys)_{18} - 5H + 2Na]^{3-}$ (#3), and $[Au_{25}(Cys)_{18} - 6H + 3Na]^{3-}$ (#4). It should be mentioned that no CTAB molecules were detected from our Cys-Au NCs in water, which indicates the complete removal of protecting layer of CTAB molecules from the Au NC surface during their phase transfer from toluene to water.

A representative transmission electron microscopy (TEM) image (Figure S1 of the Supporting Information) suggests that our $Au_{25}(Cys)_{18}$ NCs had size below 1.5 nm. The oxidation state of $Au_{25}(Cys)_{18}$ NCs was determined by X-ray photoelectron spectroscopy (XPS). As shown in Figure S2 of the Supporting Information, the Au $4f_{7/2}$ binding energies of our $Au_{25}(Cys)_{18}$ NCs (black line) are located between that of Cys-Au^I complexes (prepared by mixing $HAuCl_4$ with Cys, blue line) and Au^0 film (red line). A ~0.55 eV shift in the Au $4f_{7/2}$ binding energy from that of Au^0 film is attributed to the electron donation from Au NCs to the surface thiolates.[8]

The CTAB layer on Cys-Au^I complexes provides an effective protection for the reduction of latter by $NaBH_4$, which is the key to the direct formation of $Au_{25}(Cys)_{18}$ NCs in our protocol. It is well known that CTAB forms well-defined micelles or inverse-micelles in water or toluene due to its small headgroup and straight hydrocarbon tail.[45,46] In our reaction system, Cys-Au^I complexes are confined inside the CTAB layer via the electrostatic interaction between CTA^+ cations and carboxyl anions in Cys. The good steric hindrance of the CTAB layer leads to the formation of well-defined CTAB-protected Cys-Au^I complex inverse-micelles, which upon the reduction form $Au_{25}(Cys)_{18}$ NCs inside the CTAB template. Without the addition of CTAB in our reaction system (while keeping the other reaction conditions as constant), only a mixture of Au NCs was obtained, as evidenced by its featureless absorption spectrum (Figure S3 of the Supporting Information). Therefore, the construction of well-defined inverse-micelles is crucial for the direct formation of $Au_{25}(Cys)_{18}$ NCs in our reaction system. In addition, if we replaced CTAB by tetraoctylammonium bromide (TOAB) with four hydrocarbon tails and used the same reaction conditions, then we could only produce mixed-size Cys-Au NCs, which also show a characteristic featureless absorption spectrum (Figure S4 of the Supporting Information). The difference in the CTAB and TOAB system can be understood from their molecule structure, where the patulous molecule volume of TOAB (from four hydrocarbon tails) most likely leads to the construction of an ill-defined inverse-micelle, which results in the formation of mixed-size Cys-Au NCs.

The addition of NaOH to the reaction mixture also affects the formation of $Au_{25}(Cys)_{18}$ NCs, which is another supportive evidence of the importance of well-defined inverse-micelles in our synthesis protocol. The introduction of a certain amount of NaOH can enhance the electrostatic interaction between CTA^+ and COO^- (from Cys-Au^I complexes), which can improve the formation of well-defined inverse-micelles. If no NaOH was added to the reaction solution, then the relatively weak electrostatic interaction between CTA^+ and COO^- led to the formation of ill-defined inverse-micelles, and only mixed-size Cys-Au NCs were produced. As shown in Figure 2a (black line), a featureless absorption spectrum was observed for Cys-Au NCs synthesized in the absence of NaOH. However, the addition of a certain amount of NaOH (e.g., 350 or 500 μL, 1 M) can significantly improve the quality of the protecting CTAB layer (or inverse-micelles), thus leading to the formation of high-purity $Au_{25}(Cys)_{18}$ NCs inside the protecting layer (red line (for 350 μL of 1 M NaOH) and blue line (for 500 μL of 1 M NaOH)). The well-defined inverse-micelles provide efficient protection for Cys-Au^I complexes for the $NaBH_4$ reduction owing to their good steric hindrance, which confines the formation of $Au_{25}(Cys)_{18}$ NCs inside the CTAB layer.

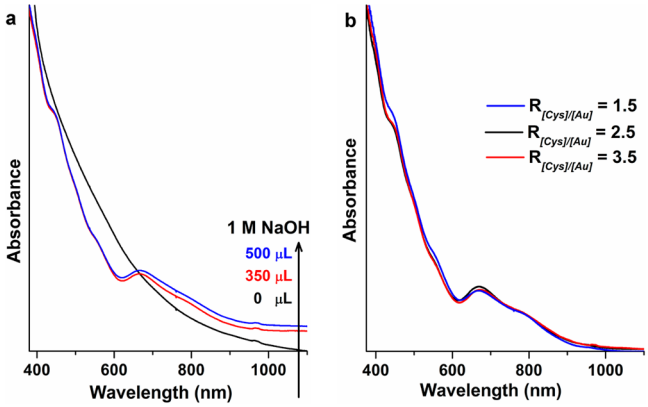

Figure 2. Effects of (a) the amount of NaOH addition and (b) the concentration ratio of thiolate ligands to Au ions ($R_{[thiolate]/[Au]}$) on the formation of Cys-Au_{25} NCs.

The synthesis strategy by using the protection−deprotection scheme is facile and robust. No strict reaction conditions (e.g., precursor concentrations and stirring speed) were required in our synthesis. For example, the concentration ratio of thiolate ligands to Au ions, $R_{[thiolate]/[Au]}$, has been reported as a common factor to affect the formation of atomically precise Au NCs.[27−29,47] However, in our reaction system, the $R_{[thiolate]/[Au]}$ value has much less effect on the formation of $Au_{25}(Cys)_{18}$ NCs. As shown in Figure 2b, with the addition of the same amount of NaOH (e.g., 1 M, 350 μL), the optical absorption spectra of Cys-Au NCs synthesized with different $R_{[thiolate]/[Au]}$ from 1.5 to 3.5 are nearly identical. All absorption spectra suggest the formation of high purity $Au_{25}(Cys)_{18}$ NCs. Our synthesis protocol for $Au_{25}(Cys)_{18}$ NCs is also insensitive to the

dx.doi.org/10.1021/jz300960b | J. Phys. Chem. Lett. 2012, 3, 2310−2314

stirring speed, which was, however, indicated in other reaction systems as a critical factor for high-purity Au_{25} NCs. As shown in Figure S5 of the Supporting Information, crude Au NC products prepared under different stirring speed from 600 to 1500 rpm exhibit almost the same absorption features as that of $Au_{25}(Cys)_{18}$ NCs. In addition, our synthesis protocol is easily scalable (e.g., to 500 mL, Figure S6 of the Supporting Information) and has excellent reproducibility in terms of product quality.

The synthesis strategy developed in this study is also fairly generic and can be easily adopted to synthesize Au_{25} NCs protected by other thiolate ligands. As a proof-of-concept, a small thiolate ligand, 3-mercaptopropionic acid (MPA), was chosen as the protecting ligand. As shown in Figure 3a, the as-

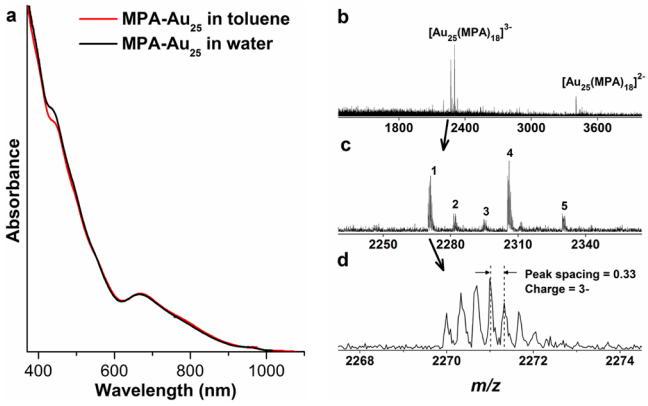

Figure 3. (a) UV−vis spectra of the as-synthesized MPA-Au_{25} NCs in toluene (red line) and in water (black line). (b−d) ESI mass spectra of the as-synthesized MPA-Au_{25} NCs in water (in negative ion mode). The species identified in panel c are $[Au_{25}(MPA)_{18} - 3H]^{3-}$ (#1), $[Au_{25}(MPA)_{18} - 4H + K]^{3-}$ (#2), $[Au_{25}(MPA)_{18} - 5H + 2K]^{3-}$ (#3), $[Au_{25}(MPA)_{18} - 6H + 3K]^{3-}$ (#4), and $[Au_{25}(MPA)_{18} - 9H + 3K + 3Na]^{3-}$ (#5).

synthesized MPA-Au NCs in toluene (CTAB-protected, red line) and in water (CTAB-deprotected, black line) exhibit the same absorption features as that of Cys-Au_{25} NCs (Figure 1a). ESI mass spectra (Figure 3b−d) of MPA-Au NCs suggest its molecule formula to be $Au_{25}(MPA)_{18}$. A representative TEM image (Figure S7 of the Supporting Information) indicates that the MPA-Au NCs were below 1.5 nm. Similar to the synthesis of $Au_{25}(Cys)_{18}$ NCs, the addition of a certain amount of NaOH is also crucial for the formation of high purity $Au_{25}(MPA)_{18}$ NCs (Figure S8 of the Supporting Information), and the $R_{[thiolate]/[Au]}$ ratio has negligible effects on the formation of $Au_{25}(MPA)_{18}$ NCs (Figure S9 of the Supporting Information).

In summary, we have developed a new synthesis strategy by using a simple protection−deprotection sequence to prepare atomically precise thiolated Au NCs. Our synthesis strategy integrated the unique thiolate−Au interactions and the steric hindrance of a removable template (CTAB) into one protocol, which has been demonstrated to be a fast (<10 min), simple, facile, and robust synthesis protocol for high-purity thiolated Au_{25} NCs. A CTAB layer was simply introduced in our reaction system to protect the thiolate-Au^{I} complexes during the $NaBH_4$ reduction, which controlled the formation rate of Au NCs inside the CTAB template, thus leading to the direct formation of thiolated Au_{25} NCs. The protecting layer can be easily removed from the NC surface once its mission was accomplished. The protection−deprotection strategy developed in this study opens a new door for the synthesis of high-quality metal NCs, which could also be extended to synthesize monodisperse metal nanoparticles.

■ ASSOCIATED CONTENT

Supporting Information

Instrumentation used and details of experimental procedures and additional figures. This material is available free of charge via the Internet at http://pubs.acs.org.

■ AUTHOR INFORMATION

Corresponding Author

*E-mail: chexiej@nus.edu.sg. Tel: +65 6516 1067.

Notes

The authors declare no competing financial interest.

■ ACKNOWLEDGMENTS

This work is financially supported by the Ministry of Education, Singapore, under grants R-279-000-295-133 and R-279-000-327-112. X.Y. acknowledges the National University of Singapore for his research scholarship.

■ REFERENCES

(1) Wuts, P. G. M.; Greene, T. W. The Role of Protective Groups in Organic Synthesis. In *Greene's Protective Groups in Organic Synthesis*, John Wiley & Sons, Inc.: Hoboken, NJ, 2006, pp 1−15.

(2) Jarowicki, K.; Kocienski, P. Protecting Groups. *J. Chem. Soc., Perkin Trans. 1* **1998**, 4005−4037.

(3) Sartori, G.; Ballini, R.; Bigi, F.; Bosica, G.; Maggi, R.; Righi, P. Protection (and Deprotection) of Functional Groups in Organic Synthesis by Heterogeneous Catalysis. *Chem. Rev.* **2003**, *104*, 199−250.

(4) Jin, R. Quantum Sized, Thiolate-Protected Gold Nanoclusters. *Nanoscale* **2010**, *2*, 343−362.

(5) Zhang, Q. B.; Xie, J. P.; Yu, Y.; Lee, J. Y. Monodispersity Control in the Synthesis of Monometallic and Bimetallic Quasi-Spherical Gold and Silver Nanoparticles. *Nanoscale* **2010**, *2*, 1962−1975.

(6) Shang, L.; Dong, S.; Nienhaus, G. U. Ultra-Small Fluorescent Metal Nanoclusters: Synthesis and Biological Applications. *Nano Today* **2011**, *6*, 401−418.

(7) Negishi, Y.; Takasugi, Y.; Sato, S.; Yao, H.; Kimura, K.; Tsukuda, T. Magic-Numbered Au_n Clusters Protected by Glutathione Monolayers (n = 18, 21, 25, 28, 32, 39): Isolation and Spectroscopic Characterization. *J. Am. Chem. Soc.* **2004**, *126*, 6518−6519.

(8) Negishi, Y.; Nobusada, K.; Tsukuda, T. Glutathione-Protected Gold Clusters Revisited: Bridging the Gap between Gold(I)−Thiolate Complexes and Thiolate-Protected Gold Nanocrystals. *J. Am. Chem. Soc.* **2005**, *127*, 5261−5270.

(9) Bakr, O. M.; Amendola, V.; Aikens, C. M.; Wenseleers, W.; Li, R.; Dal Negro, L.; Schatz, G. C.; Stellacci, F. Silver Nanoparticles with Broad Multiband Linear Optical Absorption. *Angew. Chem., Int. Ed.* **2009**, *48*, 5921−5926.

(10) Chen, S.; Ingram, R. S.; Hostetler, M. J.; Pietron, J. J.; Murray, R. W.; Schaaff, T. G.; Khoury, J. T.; Alvarez, M. M.; Whetten, R. L. Gold Nanoelectrodes of Varied Size: Transition to Molecule-Like Charging. *Science* **1998**, *280*, 2098−2101.

(11) Murray, R. W. Nanoelectrochemistry: Metal Nanoparticles, Nanoelectrodes, and Nanopores. *Chem. Rev.* **2008**, *108*, 2688−2720.

(12) Laaksonen, T.; Ruiz, V.; Liljeroth, P.; Quinn, B. M. Quantised Charging of Monolayer-Protected Nanoparticles. *Chem. Soc. Rev.* **2008**, *37*, 1836−1846.

(13) Diez, I.; Ras, R. H. A. Fluorescent Silver Nanoclusters. *Nanoscale* **2011**, *3*, 1963−1970.

(14) Lu, Y.; Chen, W. Sub-Nanometre Sized Metal Clusters: From Synthetic Challenges to the Unique Property Discoveries. *Chem. Soc. Rev.* **2012**, *41*, 3594−3623.

(15) Choi, S.; Dickson, R. M.; Yu, J. Developing Luminescent Silver Nanodots for Biological Applications. *Chem. Soc. Rev.* **2012**, *41*, 1867−1891.
(16) Shiang, Y.-C.; Huang, C.-C.; Chen, W.-Y.; Chen, P.-C.; Chang, H.-T. Fluorescent Gold and Silver Nanoclusters for the Analysis of Biopolymers and Cell Imaging. *J. Mater. Chem.* **2012**, *22*, 12972−12982.
(17) Yuan, X.; Luo, Z.; Zhang, Q.; Zhang, X.; Zheng, Y.; Lee, J. Y.; Xie, J. Synthesis of Highly Fluorescent Metal (Ag, Au, Pt, and Cu) Nanoclusters by Electrostatically Induced Reversible Phase Transfer. *ACS Nano* **2011**, *5*, 8800−8808.
(18) Zhu, Y.; Qian, H.; Drake, B. A.; Jin, R. Atomically Precise $Au_{25}(SR)_{18}$ Nanoparticles as Catalysts for the Selective Hydrogenation of α,β-Unsaturated Ketones and Aldehydes. *Angew. Chem., Int. Ed.* **2010**, *49*, 1295−1298.
(19) Nie, X.; Qian, H.; Ge, Q.; Xu, H.; Jin, R. CO Oxidation Catalyzed by Oxide-Supported $Au_{25}(SR)_{18}$ Nanoclusters and Identification of Perimeter Sites as Active Centers. *ACS Nano* **2012**, *6*, 6014−6022.
(20) Negishi, Y.; Sakamoto, C.; Ohyama, T.; Tsukuda, T. Synthesis and the Origin of the Stability of Thiolate-Protected Au_{130} and Au_{187} Clusters. *J. Phys. Chem. Lett.* **2012**, 1624−1628.
(21) Schaaff, T. G.; Knight, G.; Shafigullin, M. N.; Borkman, R. F.; Whetten, R. L. Isolation and Selected Properties of a 10.4 kDa Gold:Glutathione Cluster Compound. *J. Phys. Chem. B* **1998**, *102*, 10643−10646.
(22) Schaaff, T. G.; Whetten, R. L. Giant Gold−Glutathione Cluster Compounds: Intense Optical Activity in Metal-Based Transitions. *J. Phys. Chem. B* **2000**, *104*, 2630−2641.
(23) Tracy, J. B.; Kalyuzhny, G.; Crowe, M. C.; Balasubramanian, R.; Choi, J.-P.; Murray, R. W. Poly(Ethylene Glycol) Ligands for High-Resolution Nanoparticle Mass Spectrometry. *J. Am. Chem. Soc.* **2007**, *129*, 6706−6707.
(24) Parker, J. F.; Fields-Zinna, C. A.; Murray, R. W. The Story of a Monodisperse Gold Nanoparticle: $Au_{25}L_{18}$. *Acc. Chem. Res.* **2010**, *43*, 1289−1296.
(25) Schaaff, T. G.; Whetten, R. L. Controlled Etching of Au:SR Cluster Compounds. *J. Phys. Chem. B* **1999**, *103*, 9394−9396.
(26) Shichibu, Y.; Negishi, Y.; Tsukuda, T.; Teranishi, T. Large-Scale Synthesis of Thiolated Au_{25} Clusters *via* Ligand Exchange Reactions of Phosphine-Stabilized Au_{11} Clusters. *J. Am. Chem. Soc.* **2005**, *127*, 13464−13465.
(27) Zhu, M.; Lanni, E.; Garg, N.; Bier, M. E.; Jin, R. Kinetically Controlled, High-Yield Synthesis of Au_{25} Clusters. *J. Am. Chem. Soc.* **2008**, *130*, 1138−1139.
(28) Wu, Z.; MacDonald, M. A.; Chen, J.; Zhang, P.; Jin, R. Kinetic Control and Thermodynamic Selection in the Synthesis of Atomically Precise Gold Nanoclusters. *J. Am. Chem. Soc.* **2011**, *133*, 9670−9673.
(29) Zhu, M.; Qian, H.; Jin, R. Thiolate-Protected $Au_{24}(SC_2H_4Ph)_{20}$ Nanoclusters: Superatoms or Not? *J. Phys. Chem. Lett.* **2010**, *1*, 1003−1007.
(30) Qian, H.; Zhu, M.; Wu, Z.; Jin, R. Quantum Sized Gold Nanoclusters with Atomic Precision. *Acc. Chem. Res.* **2012**, DOI: 10.1021/ar200331z.
(31) Qian, H.; Zhu, Y.; Jin, R. Size-Focusing Synthesis, Optical and Electrochemical Properties of Monodisperse $Au_{38}(SC_2H_4Ph)_{24}$ Nanoclusters. *ACS Nano* **2009**, *3*, 3795−3803.
(32) Kumar, S.; Jin, R. Water-Soluble $Au_{25}(Capt)_{18}$ Nanoclusters: Synthesis, Thermal Stability, and Optical Properties. *Nanoscale* **2012**, *4*, 4222−4227.
(33) Jin, R.; Qian, H.; Wu, Z.; Zhu, Y.; Zhu, M.; Mohanty, A.; Garg, N. Size Focusing: A Methodology for Synthesizing Atomically Precise Gold Nanoclusters. *J. Phys. Chem. Lett.* **2010**, *1*, 2903−2910.
(34) Xie, J. P.; Zheng, Y. G.; Ying, J. Y. Protein-Directed Synthesis of Highly Fluorescent Gold Nanoclusters. *J. Am. Chem. Soc.* **2009**, *131*, 888−889.
(35) Xie, J.; Zheng, Y.; Ying, J. Y. Highly Selective and Ultrasensitive Detection of Hg^{2+} Based on Fluorescence Quenching of Au Nanoclusters by Hg^{2+}-Au^{+} Interactions. *Chem. Commun.* **2010**, *46*, 961−963.
(36) Chaudhari, K.; Xavier, P. L.; Pradeep, T. Understanding the Evolution of Luminescent Gold Quantum Clusters in Protein Templates. *ACS Nano* **2011**, *5*, 8816−8827.
(37) Chen, T.-H.; Tseng, W.-L. (Lysozyme Type VI)-Stabilized Au_8 Clusters: Synthesis Mechanism and Application for Sensing of Glutathione in a Single Drop of Blood. *Small* **2012**, *8*, 1912−1919.
(38) Duan, H.; Nie, S. Etching Colloidal Gold Nanocrystals with Hyperbranched and Multivalent Polymers: A New Route to Fluorescent and Water-Soluble Atomic Clusters. *J. Am. Chem. Soc.* **2007**, *129*, 2412−2413.
(39) Zheng, J.; Petty, J. T.; Dickson, R. M. High Quantum Yield Blue Emission From Water-Soluble Au_8 Nanodots. *J. Am. Chem. Soc.* **2003**, *125*, 7780−7781.
(40) Yang, J.; Lee, J. Y.; Ying, J. Y. Phase Transfer and Its Applications in Nanotechnology. *Chem. Soc. Rev.* **2011**, *40*, 1672−1696.
(41) Yang, J.; Ying, J. Y. A General Phase-Transfer Protocol for Metal Ions and Its Application in Nanocrystal Synthesis. *Nat. Mater.* **2009**, *8*, 683−689.
(42) Wei, Y. F.; Yang, J.; Ying, J. Y. Reversible Phase Transfer of Quantum Dots and Metal Nanoparticles. *Chem. Commun.* **2010**, *46*, 3179−3181.
(43) Yuan, X.; Yeow, T. J.; Zhang, Q.; Lee, J. Y.; Xie, J. Highly Luminescent Ag^{+} Nanoclusters for Hg^{2+} Ion Detection. *Nanoscale* **2012**, *4*, 1968−1971.
(44) Wu, Z.; Lanni, E.; Chen, W.; Bier, M. E.; Ly, D.; Jin, R. High Yield, Large Scale Synthesis of Thiolate-Protected Ag_7 Clusters. *J. Am. Chem. Soc.* **2009**, *131*, 16672−16674.
(45) Eastoe, J.; Hollamby, M. J.; Hudson, L. Recent Advances in Nanoparticle Synthesis with Reversed Micelles. *Adv. Colloid Interface Sci.* **2006**, *128−130*, 5−15.
(46) Zhang, S.; Zhao, Y. Facile Preparation of Organic Nanoparticles by Interfacial Cross-Linking of Reverse Micelles and Template Synthesis of Subnanometer Au−Pt Nanoparticles. *ACS Nano* **2011**, *5*, 2637−2646.
(47) Wu, Z.; Suhan, J.; Jin, R. One-Pot Synthesis of Atomically Monodisperse, Thiol-Functionalized Au_{25} Nanoclusters. *J. Mater. Chem.* **2009**, *19*, 622−626.